ELSEVIER

Journal of Photochemistry and Photobiology A: Chemistry 153 (2002) 135–143

Journal of Photochemistry and Photobiology A:Chemistry

www.elsevier.com/locate/jphotochem

# New fluorescent probes for monitoring the polymerization reaction: *p*-vinyliden derivatives of *N*,*N*-dimethylaminoaryl compounds

P. Bosch*, A. Fernández-Arizpe, J.L. Mateo, F. Catalina, C. Peinado

*Institute of Polymers, CSIC, Juan de la Cierva 3, 28006 Madrid, Spain*

Received 26 June 2002; accepted 1 July 2002

Dedicated to Professor J.L. Mateo on the occasion of his 70th birthday.

**Abstract**

The fluorescence emission of two new fluorescent probes have been studied in environments of different polarity and viscosity. The probes have been shown to be sensitive to changes in both microviscosity and micropolarity of the surroundings, and their dipolar moments in the excited state have been estimated. They have been used as fluorescent sensors to monitor the photopolymerization reactions of some mono- and di-functional (meth)acrylate monomers, and two commercial photocurable acrylic adhesives. The fluorescence emission band of the probes showed an increase in intensity as the degree of conversion increases, throughout the entire polymerization range in the different systems checked. Their sensitivity have been compared with that of their parent compound *N*,*N*-dimethylamino-bencilidenenmalononitrile.


*Keywords:* Fluorescent probes; Photopolymerization; Microviscosity; Micropolarity; Cure monitoring

## 1. Introduction

Photopolymerization reactions have become among the most rapidly growing in the coating industry because the processes are solvent free, the monomers are easy to formulate and the manufacturing of photosystems require less energy than the alternatives [1]. The mechanical and chemical properties of photoformed coatings are related to various factors [2], among which one of the most important is the degree of cure. As a result, techniques for monitoring the degree of cure have been a priority in the coating industry for many years, as a tool for quality control and process optimization. Several methods have been developed to study the kinetics of photopolymerization reactions, being photo-DSC and FTIR the most used. However, none of them are applicable to follow processes on-line. In contrast, fluorescence spectroscopy is both sensitive and selective, and can be used for nondestructive analysis of polymerization processes both on-line and off-line.

There are increasing literature reports describing fluorescent probes for testing processes occurring during polymerization. Probe fluorescence changes accompanying polymerization are related to both changes in the microviscosity and the local polarity of the probe induced by both the solid polymers and the resulting polymeric solutions.

The three families of fluorescence probes usually employed for sensing these processes are: (i) compounds that form excited state dimers (excimers), which have different fluorescence emission that the single molecule (usually pyrene and its derivatives) [3]; (ii) systems that could undergo energy transfer between two chromophores, such as the quenching of an excited state by a quencher [4–7]; and (iii) a single probe exhibiting multiple fluorescences depending on the environment. The mechanisms (i) and (ii) need two probe molecules to move through the medium to be sufficiently close to either form an excimer or transfer the energy, and then the processes are viscosity-dependent.

The third family uses the property of some compounds of having more than one excited state, being fluorescent at least one of them, and being the transition between the excited states done by rotation of one group around a single bond [8]. Fluorescence is then rotation-dependent, and the properties of microenvironment determine the fluorescence quantum yield and the positions of the fluorescence maxima for these compounds. *N*,*N*-dialkylarylamine derivatives with various acceptor substituents [9] exhibit photoinduced intramolecular charge-transfer (ICT) and *N*,*N*-dialkylaniline derivatives exhibit dual emissions [10].

* Corresponding author. Tel.: +34-91-562-2900; fax: +34-91-564-4853.
*E-mail address:* pbosch@ictp.csic.es (P. Bosch).

1010-6030/02/$ – see front matter 
PII: S1010-6030(02)00260-5

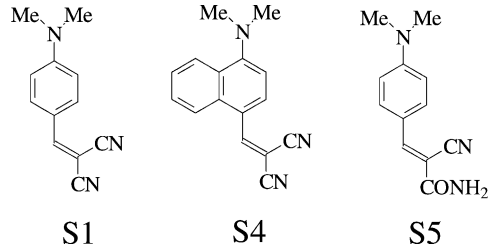


Scheme 1. Structures of the probes S1, S4 and S5.

There are several requirements that fluorescent probes must meet to be useful for monitoring polymerization reactions. The probe should have a high absorption coefficient, high fluorescence quantum yield and large Stokes shift to avoid fluorescence self-absorption. In addition, if the probe is to be used for following photoinduced polymerizations the absorption of the probe should not interfere with the absorption of the photoinitiator and the probe should be photochemically stable under curing conditions (irradiation wavelength and irradiation time). There are several studies in the literature concerning fluorescence monitoring of photopolymerization processes, most of them by Neckers and co-workers [11] but very few of the studied probes fulfill all the requirements stated above at the same time that show enough sensitivity to follow the photopolymerization reaction throughout the entire conversion range.

We present in this work two new fluorescent probes which can be used to follow photopolymerization processes until limiting conversion. The aim of the work is to study the influence of the structure of the probes in their sensing properties. The properties of the new probes have been compared with those of the classical *N,N*-dimethylamino-bencilidenemalononitrile (Loutfy's probe [12], hereafter S1) (Scheme 1).

## 2. Experimental part

### 2.1. Materials

Monomers (LA, lauryl acrylate; HDDA, hexanedioldiacrylate; and HDDMA, hexanedioldimethacrylate) were purchased from Aldrich and used without further purification.

Photoinitiator 2,2-dimethoxy-2-phenylacetophenone (DMPA, trademark Irg651®) provided by Ciba SC, and adhesives L329 and L312 (trademark Loctite 329® and Loctite 312®) provided by Loctite España were used as received. The adhesive complete characterization were carried out by conventional techniques and their compositions determined (L329: chlorosulfonated polyethylene, methyl methacrylate, methacrylic acid, hydroxypropyl methacrylate. L312: polyurethane–methacrylate resin, hydroxypropyl methacrylate, acrylic acid).

### 2.2. Synthesis

*N,N*-dimethylamino-benzilidenemalononitrile (S1) was synthesized and purified according to procedure described before [13]. The new probe *N,N*-dimethylamino-4-(2-cyano-2-acetamidovinyl)-naphthalene (S4) was synthesized as recently described by Bosch et al. [14].

*N,N*-dimethylamino-4-(2-cyano-2-acetamidovinyl)-benzene (S5) was synthesized following the same procedure, using 0.5 g (3.35 mmol) of *p-N,N*-dimethylamino-benzaldehyde and 0.336 g (4 mmol) of cyanoacetamide dissolved in 15 ml of methanol. The mixture is stirred at 70 °C under argon as 0.2 ml of a saturated solution of sodium methoxyde in methanol were slowly added. The reaction was maintained under reflux during 10 min, until the heavy precipitation of orange crystals finished. The mixture was then cooled in an ice bath, filtered and the precipitate recrystallized from ethanol/toluene (8:2). Isolated yield: 72%.

$^{1}$H RMN ($\delta_{ppm}$, $CDCl_3$): 8.18 (s, 1H, –C=C<u>H</u>–); 7.90 (d, 2H, <u>H</u>-*meta*); 6.69 (d, 2H, <u>H</u>-*ortho*); 6.2 (s, 1H, CON<u>H</u>$_2$); 5.72 (s, 1H, CON<u>H</u>$_2$); 3.1 (s, 6H, –N(C<u>H</u>$_3$)$_2$).

$^{13}$C RMN ($\delta_{ppm}$, $CDCl_3$): 177.3; 166.5; 146.1; 135.0; 134.7; 124.8; 106.5; 53.1.

IR (KBr, cm$^{-1}$): 3450–3100 (N–H st); 2190 (CN st); 1690 ($CONH_2$ st); 1530 ($C_{Ar}$–C st); 1350 (–N($CH_3$)$_2$ $\delta$ si); 780 (C=C $\delta$ oop).

### 2.3. Spectral measurements

Solvents were analytical grade (Merck, Aldrich) and were used without further purification. Absorption spectra were recorded with a Perkin-Elmer UV–VIS Lambda 16 spectrophotometer. Fluorescence spectra were taken on a Perkin-Elmer LS 50B spectrophotometer using the absorption maximum wavelength as the excitation wavelength and varying the slits in order to achieve a better spectra for the different probes. Fluorescence quantum yields were determined by comparing with the usual standard 9,10-diphenylanthracene fluorescence in cyclohexane. The optical densities of all the probes were in the range 0.3–1.0 at the absorption maximum.

### 2.4. Cure proceeding and analysis

#### 2.4.1. Photopolymerization of monomers

The fluorescent probe (0.02% w/w) and photoinitiator (0.5–1% w/w) were dissolved in the monomer to be studied. Then, 40 mg of this formulation were placed into an aluminium pan for the photo-DSC measurements (sample thickness 0.6 mm). Samples were irradiated under nitrogen in situ with a MACAM-Flexicure portable irradiation system provided with a Sylvania 400 W Hg medium-pressure lamp and twin quartz optical fiberguides. The procedure for photo-DSC analysis has been described previously [15]. Incident light intensity was set constant for all runs at a

value of 0.5 mcal $s^{-1}$. Immediately after reaching a given conversion, the sample pan was placed into the fluorimeter sample holder and the fluorescence spectrum was acquired.

#### 2.4.2. Photopolymerization of adhesives

Samples containing probe (0.03% w/w), photoinitiator (1% w/w) and the adhesive formulation were prepared by stirring in the dark all components until homogeneous solutions were obtained (not less than 8 h). The photocurable formulations were applied as an uniform layer coating on an aluminium foil and covered with a low density polyethylene film (LDPE, of 40 μm thickness) for the RT-FTIR experiments, or between two LDPE films for the laser experiments. Photosensitive coatings of 10 μm thickness were obtained by controlled pressing.

Samples were photopolymerized at room temperature under air atmosphere until their limiting conversion. The irradiation source was a Sylvania 400 W Hg medium-pressure lamp (MACAM-Flexicure portable system provided with a quartz optical fiberguide) which provided polychromatic continuous light. For all samples, the disappearance of double bonds have been monitored in situ by means of RT-FTIR, following the decrease of the 817 $cm^{-1}$ band corresponding to the out of the plane deformation of the acrylate double bond. The changes in the fluorescence of the probes as photopolymerization proceeds have been followed by real time luminescence spectroscopy, using a Nd-YAG pulsed laser (Quanta-Ray from Spectra Physics) emitting at 355 nm as excitation beam and an intensified Charge Coupling Device (Andor camera ICCD-408) as detector. Complete description of the experimental setup has been described recently [16].

### 2.5. Steady-state irradiation

Degassified samples were irradiated with the white light coming from the Macam-Flexicure system. Disappearance of the probes during irradiation was followed by UV spectroscopy at the maximum wavelength of the charge-transfer absorption band, in a Shimatzu UV-256 FS spectrophotometer.

### 2.6. Dipole moment determination

In order to determine the excited state singlet dipole moments by the solvatochromic method, the Bakhshiev's formula [17] was used:

$$\bar{\nu}_A - \bar{\nu}_F = \frac{2(\mu_e - \mu_g)^2}{hca_0^3} F_1 \quad (1)$$

where $\bar{\nu}_A$ and $\bar{\nu}_F$ are the wavenumbers ($cm^{-1}$) of the absorption and emission maxima respectively, $\mu_g$ and $\mu_e$ are the permanent dipole moments in the ground and first excited states respectively, $a_0$ is the Onsager cavity radius and $F_1$ is the solvent polarity function defined as follows:

$$F_1 = \left[\frac{D-1}{D+2} - \frac{n^2-1}{n^2+2}\right]\frac{2n^2+1}{n^2+2} \quad (2)$$

where $D$ is the solvent dielectric constant and $n$ is the solvent refractive index.

## 3. Results and discussion

### 3.1. Synthesis

The fluorescent probe S5 was prepared according to the procedures described by McKusick et al. and Sulzberg and Cotter [13] but using cyanoacetamide instead malononitrile as reactant in the condensation reaction (Scheme 2).

S4 has been synthesized following the procedure recently published by us [14].

The synthetic reactions are easy, rapid and both have high yields, being the products easy to purify. All of this makes this family of probes very suitable to be used as fluorescent sensors, because their synthesis could be easily scaled for large quantities production.

### 3.2. Absorption and emission properties

A description of the absorption and emission maxima of S5 in several solvents, together with the corresponding absorption molar coefficients are summarized in Table 1. Data for S4 have been included.

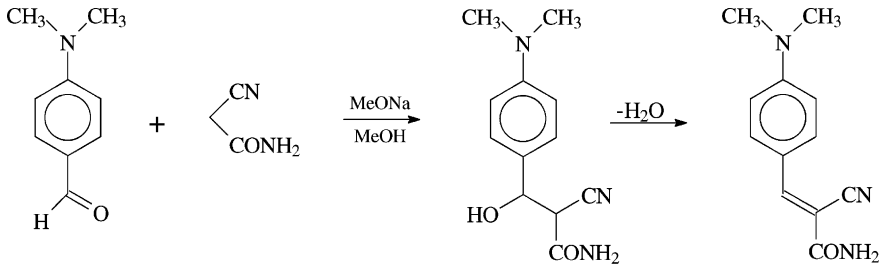


**S5**

Scheme 2. Preparation of probe S5.

Table 1
Maximum absorption and emission wavelengths, and absorption coefficients for the probes S4 and S5

| Solvent | S4[a] | | | S5 | | |
|---|---|---|---|---|---|---|
| | $\lambda_{abs}$ | $\varepsilon$ (l mol$^{-1}$ cm$^{-1}$) | $\lambda_{em}$ | $\lambda_{abs}$ | $\varepsilon$ (l mol$^{-1}$ cm$^{-1}$) | $\lambda_{em}$ |
| Cyclohexane | 428 | 246 | 490 | 386 | 306 | 440 |
| Ether | 434 | 275 | 502 | 396 | 405 | 446 |
| Chloroform | 462 | 306 | 521 | 422 | 529 | 466 |
| THF | 448 | 310 | 518 | 402 | 420 | 458 |
| Ethyl acetate | 443 | 238 | 520 | 401 | 559 | 459 |
| Acetone | 454 | 330 | 524 | 405 | 430 | 472 |
| Methanol | 450 | 242 | 525 | 412 | 377 | 479 |
| *iso*-Propanol | 451 | 250 | 524 | 409 | 385 | 468 |
| *n*-Butanol | 452 | 260 | 524 | 412 | 391 | 466 |
| Water | – | – | – | 426 | – | 475 |

[a] From Ref. [14].

The electronic absorption spectra present two main bands, whose maxima are located in the 230–280 nm and >350 nm regions. The shortest wavelength band corresponds to the $\pi \rightarrow \pi^*$ transition whereas the long-wavelength band, characterized by higher molar absorption coefficient, is attributed to the CT transition. On varying the solvent polarity, relatively long shifts in the absorption maxima are observed (up to 40 nm from cyclohexane to water). The fluorescence emission spectra of the probe show only one peak in polar solvents. The fluorescence maxima are also red shifted on increasing solvent polarity showing $\Delta\lambda$ up to 35 nm. Quantum yields of S5 in fluid media are very low ($<10^{-3}$) independently of the solvent polarity.

This behavior agrees with the data described by us for S1 and S4 and seems to be a general behavior for the cyanovinyl derivatives.

### 3.3. Excited singlet state dipole moment

The dipolar moment in the excited state for the new fluorescent probe S5 has been estimated from the value of the slope of the Bakshiev's solvatochromic plot (Eq. (1) and Fig. 1). The value of $\mu_e$ is shown in Table 2 together with the

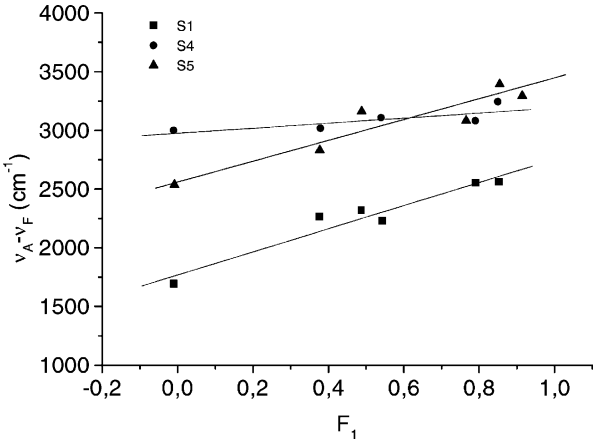


Fig. 1. Bakshiev's solvatochromic plot for the probes S1, S4 and S5.

Table 2
Calculated molecular volumes and estimated ground and excited singlet state dipole moments for the probes S1, S4 and S5

| Probe | $V$ (Å$^3$) | $\mu_g$(D) | $\mu_e$(D) |
|---|---|---|---|
| S1[a] | 198 | 6.65 | 24.0 |
| S4[a] | 244 | 8.59 | 14.7 |
| S5 | 208 | 4.05 | 14.4 |

[a] From Ref. [14].

data for its homologues S1 and S4, as well as the parameters for $V$ and $\mu_g$ calculated by semiempirical AM1 method. The assumptions taken for the calculations have been discussed before [14].

Given the lower electrowithdrawing character of the amide group in the S5 structure, respect to the cyano group in S1 and S4 structures, the dipolar moments in both the ground and the excited states for S5 are lower than the values of the malononitrile derivatives.

### 3.4. Stability of the probes under irradiation conditions

Solutions of probe ($4 \times 10^{-3}$ M) and photoinitiator ($10^{-2}$ M) in ethyl acetate have been irradiated with white light, and both S4 and S5 suffer complete photobleaching in few minutes. This is due to a rapid attack of the primary photoinitiator radicals to the vinyl double bond of the probe which causes the rupture of the conjugated D–π–A system and then the disappearance of the chromophore group.

However, when solutions of probe, photoinitiator and monomer were irradiated in ethyl acetate, complete stability of the probe was observed through invariability of the CT absorption band during prolonged irradiation ($t > 100$ min). This shows that for the process of addition of initiator radicals to vinyl or acrylic double bonds, the kinetic constant for attacking an acrylic double bond is much higher than for attacking the vinyl double bond of the probes, and then, these probes are suitable for sensing photopolymerization reactions of acrylic monomers if the concentration of monomer is higher than the concentration of probe. Giving the con-

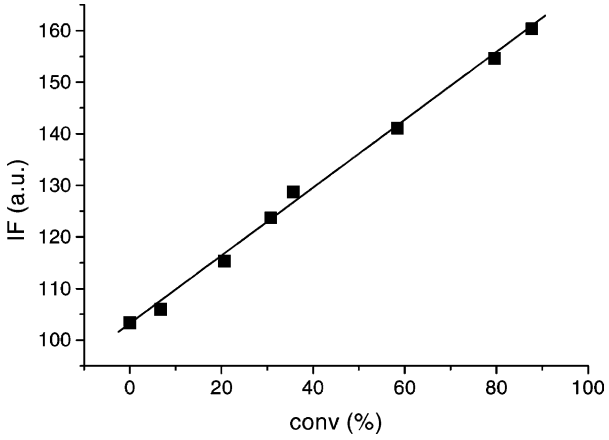


Fig. 2. Variation of fluorescence intensity of S5 versus double bond conversion during the photopolymerization reaction of lauryl acrylate.

centrations of probe employed (less than 0.05% w/w) this means that the addition of initiating radicals will take place exclusively onto the acrylic double bonds until completion of the polymerization reaction.

### 3.5. Monitoring the polymerization reaction of acrylic monomers

S4 and S5 have been checked as fluorescent probes to follow the photoinduced polymerization reaction of acrylic monomers, together with the malononitrile derivative S1. Both S4 and S5 probes suffer clear variations in the emission intensity of their fluorescence spectra along the polymerization reaction which is the same behavior showed by S1 [18]. They do not experiment variations in the position of the band, so the response of the probes towards changes in the viscosity could be directly quantified measuring the intensity of the fluorescent band at the maximum wavelength.

For the photopolymerization reaction of monofunctional acrylic monomers, S5 fluorescence shows a linear variation with the degree of polymerization followed by DSC, throughout the whole conversion range. As an example in Fig. 2 is shown the fluorescence–conversion plot for the polymerization of lauryl acrylate–S5 system.

In Fig. 3 are shown the kinetic profiles for the photoinitiated polymerization of a difunctional acrylic monomer, HDDA, obtained following the changes in fluorescence intensity of S1, S4 and S5, as well as the conversion–time plots obtained by DSC for the same reaction.

It could be seen that the evolution of the reaction is perfectly followed by the fluorescence emission of the probes, and the rate of polymerization could be obtained as the tangent to the fluorescent curve in any point.

The sensitivity of the probes, $S$, has been taken as:

$$S = \frac{\Delta IF}{IF_0} = \frac{IF_f - IF_0}{IF_0}$$

then reflecting the total change of the fluorescence for the same complete polymerization reaction. The subscripts 0

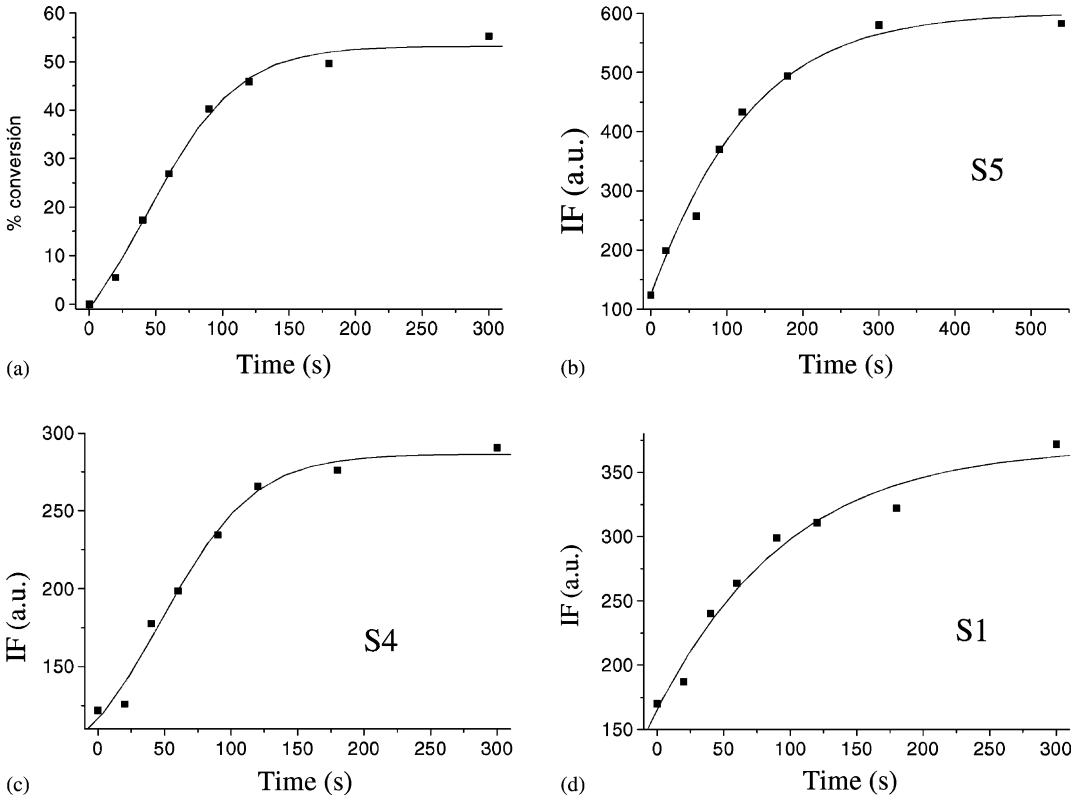


Fig. 3. (a) Conversion-time and fluorescence-time plots (b, c, d) for the photoinitiated polymerization of HDDA. $I_0 = 0.05$ mcal/s.

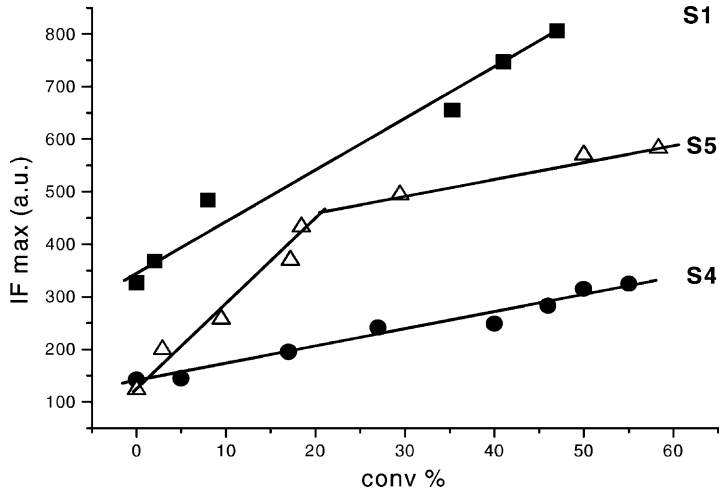


Fig. 4. Variation of fluorescence intensity of S1, S4 and S5 versus double bond conversion during the photopolymerization reaction of HDDA.

and f refer to the initial and final values of the intensity of fluorescence (IF). The sensitivity for the malononitrile derivatives S1 ($S = 1.33$) and S4 ($S = 1.5$) is somewhat similar. The presence of a naphtalene ring in S4 instead the benzene ring of S1 does not apparently affect the sensing characteristics of the probe. However, S5 results more sensitive than its homologues ($S = 2.85$). This effect has been also detected in other derivatives bearing a –CO–NH– group and there are many fluorescent sensors described with this functional group [19] and is also in accordance with previous results of our group [14,18].

The changes in fluorescence intensity of the probes have been correlated with the degree of double bond conversion (Fig. 4).

As can be seen, the plots for S1 and S4 are linear until limiting conversion, and then, the fluorescence intensity for these probes is proportional to the polymerization degree for each probe/monomer system throughout the entire polymerization range.

The response of S5 is different and show a two-slope plot with an interception point above 20% of conversion. This behavior has been recently described by us [18] and Okay et al. [20] for the polymerization reaction of multifunctional crosslinking monomers, and the interception point is related to the beginning of the gelation in which the tridimensional network is already formed and surrounds the probe.

When HDDMA is used as monomer, both S4 and S5 show a two-slope variation of the fluorescence versus double bond conversion. This is probably because a more rigid tridimensional network is obtained and then even the less sensitive probe S4 is able to detect the beginning of gelation (Fig. 5).

### *3.6. Monitoring the curing reaction of photocurable adhesive systems*

In Fig. 6 the RT-FTIR kinetic profiles for the photopolymerization of L329 are shown. Plots for L312 are similar. Two different photoinitiators (Irg651 and Irg819) have been used. The systems showed differences in rate of polymerization and limiting double bond conversion reached, depending on the difference in reactivity of the photoinitiator (higher efficiency for the phosphonyl initiating radicals [21] of Irg819) and the polymerizable monomers of the formulation (higher $k_p$ for the acrylic double bonds [22] of L312). These effects have been widely studied and described in the literature [23].

The kinetic profiles show the conventional behavior of a photocrosslinking curing reaction. Rates of polymerization have been obtained as the slope of the initial linear region and the data are compiled in Table 3, together with the limiting conversion reached. The presence of the probes does not affect the kinetic profile of the reaction in any case, so they are suitable to be used as sensors of this process.

As it happened for the polymerization reaction of the monomers, the emission spectra of the probes exhibit an

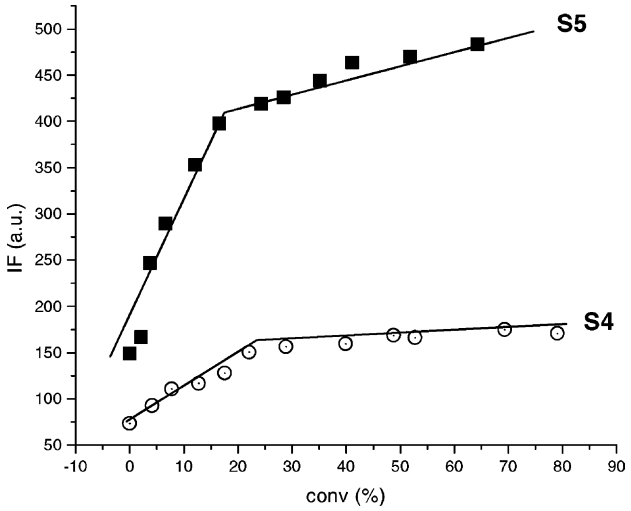


Fig. 5. Variation of fluorescence intensity of S4 and S5 versus double bond conversion during the photopolymerization reaction of HDDMA.

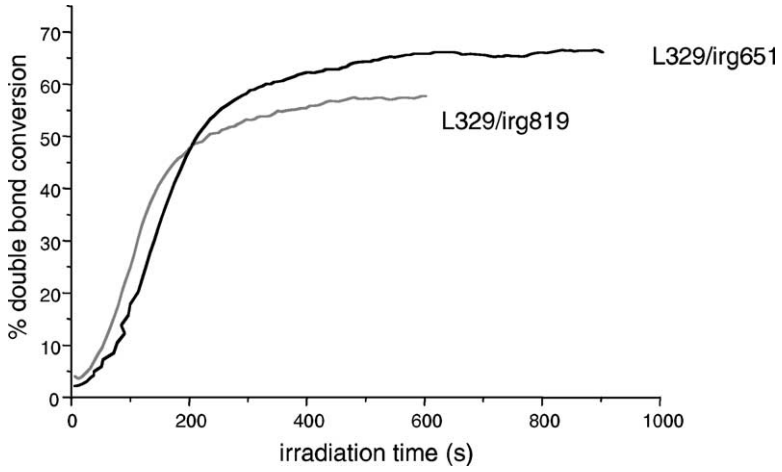


Fig. 6. Kinetic profile of the photocuring reaction of Loctite 329 using Irg651 and Irg819 as photoinitiators.

Table 3
Rates of polymerization and double bond limiting conversion for the photocuring reaction of Loctite 329 and Loctite 312. Data obtained from RT-FTIR measurements

| Adhesive | Photoinitiator | $R_p/[M]$ ($s^{-1}$) | $\alpha$ (%) |
|---|---|---|---|
| L329 | Irg651 | 0.4 | 64 |
| | Irg819 | 0.6 | 58 |
| L312 | Irg651 | 2.5 | 62 |
| | Irg819 | 4.7 | 60 |

increase in intensity during the curing reaction without changes in the position neither shape of the bands, then the changes in their fluorescence intensity versus irradiation time have been monitored as the curing of the adhesives proceeds.

The kinetic profiles obtained by fluorescence are similar to the RT-FTIR ones, showing the regions of rapid polymerization and the subsequent plateau. As the profiles for the different systems are similar, plots for L329/Irg651 and L312/Irg819 are selected as examples (Fig. 7).

The slope of the non-normalized plots for a given polymerizing system should be related with the sensitivity of each probe/adhesive system, and they are shown in Table 4. The values for the fluorescence rate of polymerization ($\rho$) have been calculated as the slopes of the normalized fluorescence–time plots and they have been also compiled in Table 4. It could be seen that the rate of polymerization measured does not depend on the probe used, which is an essential requirement for a probe to be used as sensor of the process. The new probe S4 show slightly lower sensitivity than S1 for these particular formulations, but S5 have $S$ values up to four times higher, depending on the system.

Table 4
Relative rates of polymerization ($\rho$), calculated by fluorescence, and sensitivity of the probes in the adhesive systems

| Probe | L312 | | L329 | |
|---|---|---|---|---|
| | $\rho$ ($s^{-1}$) | Sensitivity | $\rho$ ($s^{-1}$) | Sensitivity |
| S1 | 0.025 | 34 | 0.004 | 3.8 |
| S4 | 0.027 | 22 | 0.003 | 1.6 |
| S5 | 0.031 | 96 | 0.005 | 14.1 |

The variations of fluorescence with degree of double bond conversion for L312 are shown in Fig. 8. Plots for L329 are similar in shape.

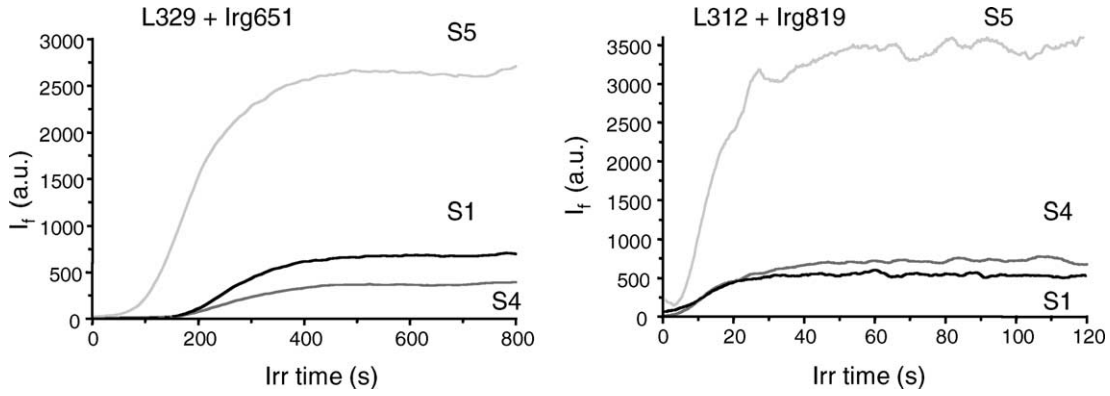


Fig. 7. Variation of fluorescence intensity of S1, S4 and S5 versus irradiation time during the photocuring reaction of Loctite 329 and Loctite 312.

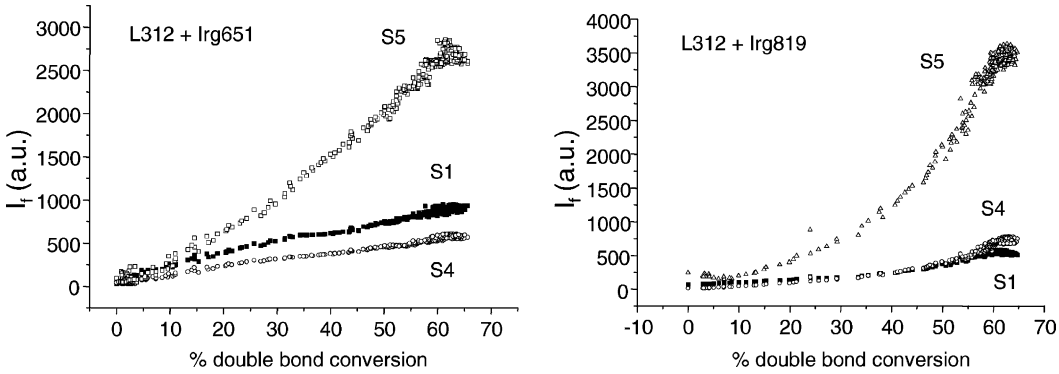


Fig. 8. Variations of fluorescence of S1, S4 and S5 with degree of double bond conversion for the photocuring reaction of Loctite 312 using Irg651 and Irg819 as photoinitiators.

As it can be seen, the three probes under study are sensitive throughout the entire range of the photopolymerization reaction, and probe S5 resulted much more sensitive to the changes in rigidity than the malononitrile derivatives S1 and S4.

The variations of $IF_{max}$ with the rigidity of the medium show a two-slope plot for the reaction when initiated by any of both photoinitiators. This is the behavior commented before for a crosslinking polymerization. But the plots are different in shape, showing different variation in rigidity for the same degree of double bond conversion depending on the photoinitiator used. The rigidity reaches higher values at the beginning of the reaction (higher value of the slope) for the system L312/Irg651. This behavior has been recently described by us for these systems using other family of fluorescent probes, and we have proposed that the different variation of the fluorescence is an evidence of the different mechanism of crosslinking reaction depending on the photoinitiator used [24]. This is due to the higher proportion of crosslinking by H-abstraction secondary reactions during the first stages of the polymerization when using Irg651, in which the hydrogen abstraction is a very important secondary reaction, and not with Irg819, in which this reaction is practically negligible. This fact, that could not be observed with RT-FTIR technique since it does not involve double bond disappearance, is clearly detected when fluorescence probes are used, and it evidences that these new fluorescent probes are useful for following not only the kinetics but also the mechanism of the polymerization reaction.

## 4. Conclusions

Two new fluorescent probes have been synthesized and their fluorescence emission have been characterized towards changes in the polarity and viscosity of the medium, and they have been used to monitor the polymerization reaction of mono- and di-functional acrylic and methacrylic monomers as well as the curing process of UV-curable adhesive systems. As photopolymerization proceeds, the fluorescence band of the probes showed an increase in intensity until final conversion. This behavior allows to follow the reaction by fluorescence spectroscopy.

The fluorescent kinetic profiles accurately reproduce those obtained either by photo-DSC or by RT-FTIR, showing the three steps of the crosslinking reaction: the rapid initial polymerization, gelation and the termination of the reaction due to vitrification of the system. The rate of polymerization has been measured from the fluorescence–time plots.

For crosslinking polymerization reactions, S5 probe show a two-slope variation indicating the onset of the gelation step. S4 resulted less sensitive and show this behavior only for systems undergoing high degree of crosslinking.

Differences in the mechanism taking place have been detected by fluorescence when the same system is polymerized with two different photoinitiators, reflecting the secondary crosslinking processes which take place by hydrogen abstraction. These differences could not be observed by RT-FTIR and this reflects the sensitivity of these probes and the importance of fluorescence as method to follow both the kinetics and mechanism of the polymerization reaction.

## Acknowledgements

Thanks are due to European Union Commission (Brite-EuRam Project no. 97-4472) and Comisión Interministerial de Ciencia y Tecnología (projects MAT98-0518-CE, MAT98-0518 and MAT2000-1671) for financial support. We thank to Dr. Kurt Dietliker, from Ciba Specialty Chemicals, for providing the photoinitiators, and also to Loctite España for the adhesives.

## References

[1] S.P. Pappas (Ed.), UV Curing: Science and Technology, Vol. 1, Technology Marketing Corporation, Norwalk, CT, 1978.
[2] S.P. Pappas (Ed.), UV Curing: Science and Technology, Vol. 2, Technology Marketing Corporation, Norwalk, CT, 1978.

[3] (A) F.W. Wang, R.E. Lowry, W.H. Grant, Polymer 25 (1984) 690;
(B) O. Valdés-Aguilera, C.P. Pathak, D.C. Neckers, Macromolecules 23 (1990) 689;
(C) Ö. Peckcan, Y. Yilmaz, O. Okay, Polymer 38 (1997) 1693.
[4] J.A.J. Burrows, G.W. Haggquist, R.D. Burkhart, Macromolecules 23 (1990) 988.
[5] G. Wang, L. Chen, M.A. Winnik, Macromolecules 23 (1990) 1650.
[6] F.M. Winnik, Macromolecules 23 (1990) 1647.
[7] K.E. Miller, E.L. Burch, F.D. Lewis, J.M. Torkelson, J. Polym. Sci. B Phys. 32 (1994) 2625.
[8] H. Itagaki, in: T. Tanaka (Ed.), Experimental Methods in Polymer Science, Academic Press, Massachusetts, 2000 (Chapter 3).
[9] (a) R. Hayashi, S. Tazuke, C.W. Frank, Chem. Phys. Lett. 135 (1987) 123;
(b) S. Tazuke, R.K. Guo, R. Hayashi, Macromolecules 21 (1988) 1046;
(c) S. Tazuke, R.K. Guo, R. Hayashi, Macromolecules 22 (1989) 729;
(d) M.S.A. Abdel-Mottaleb, M.Y. El-Kady, R.O. Loutfy, F.M. Winnik, J. Photochem. Photobiol. A Chem. 53 (1990) 387.
[10] (a) H.J. van Ramesdonk, M. Vos, J.W. Verhoeven, G.R. Mohlman, N.A. Tissink, A.W. Meesen, Polymer 28 (1987) 951;
(b) K.J. Shea, G.J. Stoddart, D.Y. Sasaki, Macromolecules 22 (1989) 4303;
(c) K.J. Shea, D.Y. Sasaki, G.J. Stoddart, Macromolecules 22 (1989) 1722;
(d) J. Paczkowski, Macromolecules 24 (1991) 1173.
[11] (A) J. Paczkowski, D.C. Neckers, Macromolecules 24 (1991) 3013;
(B) J. Paczkowski, D.C. Neckers, Macromolecules 25 (1992) 548;
(C) I. Kotchetov, D.C. Neckers, J. Imaging Sci. Technol. 37 (1993) 156;
(D) Z.J. Wang, J.C. Song, R. Bao, D.C. Neckers, J. Polym. Sci. B Phys. 34 (1996) 325;
(E) R. Popielarz, S. Hu, D.C. Neckers, J. Photochem. Photobiol. A Chem. 110 (1997) 79.
[12] (a) R.O. Loutfy, K.Y. Law, J. Phys. Chem. 84 (1980) 2803;
(b) R.O. Loutfy, Macromolecules 14 (1981) 270;
(c) K.Y. Law, Photochem. Photobiol. 33 (1981) 799.
[13] (a) B.C. McKusick, R.E. Hecker, J.L. Cairns, D.D. Koffman, H.F. Mower, J. Am. Chem. Soc. 80 (1958) 2806;
(b) T. Sulzberg, R.J. Cotter, Macromolecules 2 (1969) 150.
[14] P. Bosch, A. Fernández-Arizpe, J.L. Mateo, A.E. Lozano, P. Noheda, J. Photochem. Photobiol. A Chem. 133 (2000) 51.
[15] J.L. Mateo, P. Bosch, A.E. Lozano, Macromolecules 27 (1994) 7794.
[16] C. Peinado, E.F. Salvador, J. Baselga, F. Catalina, Macromol. Chem. Phys. 202 (2001) 1924.
[17] N.G. Bakhshiev, Opt. Spektrosk. 16 (1964) 821.
[18] P. Bosch, A. Fernández-Arizpe, J.L. Mateo, Macromol. Chem. Phys. 202 (9) (2001) 1961.
[19] A. Prasanna de Silva, H.Q. Nimal Gunaratne, T. Gunnlaugson, A.J.M. Huxley, C.P. McCoy, J.T. Rademacher, T.E. Rice, Chem. Rev. 97 (1997) 1515.
[20] O. Okay, D. Kaya, O. Peckan, Polymer 40 (1999) 6179.
[21] (a) T. Majima, W. Schnabel, J. Photochem. Photobiol. A 50 (1989) 31;
(b) J.E. Baxter, R.S. Davidson, H.J. Hageman, Eur. Polym. J. 24 (1988) 419;
(c) T. Sumiyoshi, W. Schnabel, Makromol. Chem. 186 (1985) 1811;
(d) T. Sumiyoshi, W. Schnabel, A. Henne, P. Lechtken, Polymer 26 (1985) 141;
(e) W. Schnabel, J. Radiat. Curing 13 (1986) 26.
[22] J. Brandrup, E.H. Immergut, E.A. Grulke (Eds.), Polymer Handbook, 4th Edition, Wiley, New York, 1999.
[23] (a) H. Fischer, R. Baer, R. Hamy, I. Verhoolen, M. Walbiner, J. Chem. Soc. Perkin II 2 (1990) 787;
(b) C.J. Groenenboom, H.J. Hageman, T. Overeem, A.J.M. Weber, Makromol. Chem. 183 (1982) 281;
(c) T. Majima, W. Schnabel, J. Photochem. Photobiol. A Chem. 50 (1989) 31;
(d) T. Sumiyoshi, W. Schnabel, Makromol. Chem. 186 (1985) 1811;
(e) J.E. Baxter, R.S. Davidson, H.J. Hageman, Polymer 29 (1988) 1569.
[24] P. Bosch, A. Fernández-Arizpe, F. Catalina, J.L. Mateo, C. Peinado, Macromol. Chem. Phys. 203 (2) (2002) 334.